

## Electronic structure and spin polarization of $\text{Mn}_x\text{Ga}_{1-x}\text{N}$

Leor Kronik, Manish Jain, and James R. Chelikowsky

*Department of Chemical Engineering and Materials Science, University of Minnesota, Minneapolis, Minnesota 55455*  
*and Minnesota Supercomputing Institute, University of Minnesota, Minneapolis, Minnesota 55455*

(Received 12 October 2001; revised manuscript received 19 April 2002; published 22 July 2002)

We present *ab initio* pseudopotential–density-functional calculations for the electronic structure of the dilute magnetic semiconductor  $\text{Mn}_x\text{Ga}_{1-x}\text{N}$ , with a realistic  $x=0.063$ , in its ordered ferromagnetic phase. We find that the introduction of Mn results in the formation of a 100% spin polarized  $\sim 1.5$  eV-wide impurity band, primarily due to hybridization of Mn  $3d$  and N  $2p$  orbitals. This band renders the material half metallic and supports effective-mass transport within it. As such,  $\text{Mn}_x\text{Ga}_{1-x}\text{N}$  is a highly suitable material for spin injectors. Coupled with the previously reported high Curie temperature and inherent compatibility with GaN technology of this material, it emerges as a serious candidate for the next generation of spintronic devices.

DOI: 10.1103/PhysRevB.66.041203

PACS number(s): 75.50.Pp, 71.55.Eq, 71.20.Nr

Dilute magnetic semiconductors (DMS's) have attracted considerable attention, because they hold the promise of using electron *spin*, in addition to its *charge*, for creating a new class of “spintronic” semiconductor devices with unprecedented functionality. The suggested applications include, e.g., “spin field effect transistors,”<sup>1</sup> which could allow for software reprogramming of the microprocessor hardware during run time, semiconductor-based “spin valves,”<sup>2</sup> which would result in high-density nonvolatile semiconductor memory chips, and even “spin qubits,”<sup>3</sup> to be used as the basic building block for quantum computing.

Over the last five years attention was paid primarily to  $\text{Mn}_x\text{Ga}_{1-x}\text{As}$ , for several reasons. First, significant breakthroughs in the nonequilibrium growth of  $\text{Mn}_x\text{Ga}_{1-x}\text{As}$ , pioneered by Ohno and co-workers,<sup>4</sup> has enabled its practical growth with stoichiometric amounts of Mn ( $x$  as high as  $\sim 0.1$ ).<sup>5</sup> Second, this material has been experimentally confirmed to be ferromagnetic, with a Curie temperature as high as 110 K.<sup>4</sup> Third,  $\text{Mn}_x\text{Ga}_{1-x}\text{As}$  alloys are inherently compatible with existing GaAs technology, resulting in the practical realization of device structures combining ferromagnetic and nonmagnetic layers.<sup>6</sup> Last, but by no means least, injection of spin-polarized holes has been observed experimentally<sup>7–9</sup> and supported theoretically,<sup>10</sup> proving that “spintronic” devices are feasible.

A significant limitation of  $\text{Mn}_x\text{Ga}_{1-x}\text{As}$ -based spintronic technology is that the Curie temperature is well below the room temperature. Dietl *et al.* predicted theoretically, based on a Zener model, that an alloy of  $\text{Mn}_x\text{Ga}_{1-x}\text{N}$ , with an amount of Mn comparable to that used in  $\text{Mn}_x\text{Ga}_{1-x}\text{As}$ , should result in a Curie temperature exceeding room temperature.<sup>11</sup> Of course, GaN is a technologically important material in its own right due to its applications in numerous devices, most notably the blue solid-state laser.<sup>12</sup> The prediction of Dietl *et al.* led to a flurry of recent experimental<sup>13–19</sup> and theoretical<sup>20–24</sup> investigations of  $\text{Mn}_x\text{Ga}_{1-x}\text{N}$ .

On the experimental side, wurtzite  $\text{Mn}_x\text{Ga}_{1-x}\text{N}$  was grown successfully by five independent groups, in microcrystalline,<sup>13</sup> bulk,<sup>14</sup> epitaxial,<sup>15,16</sup> Mn-implanted,<sup>17,18</sup> and Mn-doped<sup>19</sup> form, with an  $x$  as high as 0.005, 0.03, 0.14,<sup>15</sup> 0.1, and 0.03, respectively. The microcrystalline material was found to be paramagnetic and the epitaxial material appeared to have a Curie temperature of  $\sim 10$ –25 K. In

contrast, the ion-implanted and doped layers displayed a very high Curie temperature of  $\sim 250$  K and up to 370 K, respectively, in reasonable agreement with the theory.

On the theoretical side, Litvinov and Dugaev used a model based on virtual acceptor level—valence-band transitions to provide a detailed, quantitative prediction of the dependence of the Curie temperature on the Mn concentration, for various wurtzite III-N alloys.<sup>20</sup> Fong *et al.* used a tight-binding approach to study the Mn impurity in GaN,<sup>21</sup> Katayama-Yoshida and co-workers used the local-density approximation (LDA) to study the density of states (DOS) for ordered  $\text{Mn}_x\text{Ga}_{1-x}\text{N}$  with  $x=0.25$  (Ref. 22), and the Koringa-Kohn-Rostoker coherent potential approximation (KKR-CPA) method to study the DOS of disordered GaN with 5% of various transition metals, including Mn.<sup>23</sup> Finally, van Schilfgaarde and Myrasov used LDA to study the effect of Mn clustering in zinc blende GaN.<sup>24</sup>

As mentioned above, a successful operation of spintronic devices requires more than a ferromagnetic semiconductor. It requires the support of spin-polarized transport so that spin-polarized charge carriers may be injected into a nonmagnetic semiconductor. As opposed to  $\text{Mn}_x\text{Ga}_{1-x}\text{As}$ , to the best of our knowledge this issue has not been tackled either experimentally or theoretically for  $\text{Mn}_x\text{Ga}_{1-x}\text{N}$ . In this paper, we examine the theoretical limits to spin-polarized transport in wurtzite  $\text{Mn}_x\text{Ga}_{1-x}\text{N}$ , with a realistic  $x=0.063$ , by using first-principles calculations based on spin-polarized density-functional theory. We find that Mn  $3d$  and N  $2p$  hybridization results in an impurity band that makes the material *half metallic* and therefore ideal for spin injection. We suggest that if technological barriers can be overcome,  $\text{Mn}_x\text{Ga}_{1-x}\text{N}$  is preferable to  $\text{Mn}_x\text{Ga}_{1-x}\text{As}$  not only because of its higher Curie temperature, but also because its band structure is much more suitable for spin injection.

All calculations presented below were performed by using *ab initio* pseudopotentials within density-functional theory, with a plane-wave basis.<sup>25</sup> We employed the local-spin-density approximation, implemented using the Perdew-Wang exchange-correlation functional,<sup>26</sup> and used Troullier-Martins pseudopotentials<sup>27</sup> cast into the separable Kleinman-Bylander form.<sup>28</sup> Electron configurations of  $4s^{1.75}4p^{0.25}3d^5$  (Mn),  $2s^22p^3$  (N), and  $4s^24p^14d^0$  (Ga), with  $s/p/d$  cutoff radii (in a.u.) of 1.90/2.59/2.00, 1.50/1.50, and 2.99/2.58/

2.99, respectively, were used for generating pseudopotentials. The nonlinear partial core-correction scheme of Louie *et al.*<sup>29</sup> was used for the Mn and the Ga pseudopotentials. A plane-wave cutoff energy of 80 Ry and a  $4 \times 4 \times 4$   $k$ -point sampling scheme were used to guarantee convergence.

It is important to note that the above Ga pseudopotential does not treat the Ga 3*d* electrons as valence electrons, and treats them only implicitly via the nonlinear core correction. However, Fiorentini *et al.*<sup>30</sup> correctly noted that the Ga 3*d* electrons interact with the N 2*s* electrons, and therefore pseudopotential computations that do not consider Ga 3*d* electrons explicitly should be viewed with caution. Specifically, Fiorentini *et al.* argued that structural parameters may be underestimated and the semiconductor band gap may be overestimated. In light of this, and in order to test the quality of our pseudopotential, we also computed structural and electronic  $\text{Mn}_x\text{Ga}_{1-x}\text{N}$  properties using a  $3d^{10}4s^24p^1$  pseudopotential (with  $s/p/d$  cutoff radii of 2.19/2.19/2.19) and a plane-wave cutoff energy of 90 Ry.

Structural optimization of pure wurtzite GaN with and without explicit consideration of the Ga 3*d* electrons resulted in a lattice constant of  $a = 3.20$  Å and 3.165 Å, a  $c/a$  ratio of 1.630 and 1.620, and an internal coordinate value  $u$  of 0.3780 and 0.3775, respectively. Thus, neglecting to treat Ga 3*d* electrons explicitly results in a reasonably small 2.8% underestimate of the unit-cell volume. Both sets of numbers are in very good agreement with experiment and with previous LDA-pseudopotential calculations.<sup>31</sup>

All  $\text{Mn}_x\text{Ga}_{1-x}\text{N}$  calculations were performed within a 32-atom supercell, constructed from  $2 \times 2 \times 2$  standard unit cells of the wurtzite structure. One Ga atom was replaced with a Mn atom, resulting in  $\text{Mn}_x\text{Ga}_{1-x}\text{N}$  with  $x = 0.063$ . Because the supercell contains only one Mn atom and because the infinite crystal is constructed by exact replications of this supercell, all Mn atoms have the same neighboring atoms and possess the same spin. Therefore, the  $\text{Mn}_x\text{Ga}_{1-x}\text{N}$  phase so constructed is *ferromagnetic and ordered* by definition. This suffices for establishing the theoretical limits to spin polarization in  $\text{Mn}_x\text{Ga}_{1-x}\text{N}$ , because disorder effects (e.g., alloy disorder, Mn clustering, phase segregation, etc.), as well as the limited stability of the ferromagnetic phase, will clearly only serve to impede spin-polarized transport in these materials.

Partial density-of-states curves were computed by deconvolving the obtained wave functions over atomic orbitals of valence electrons. Spheres of  $\sim 1.3$  Å,  $\sim 1.3$  Å, and  $\sim 0.8$  Å for Mn, Ga, and N, respectively, centered around each atom, were used for the deconvolution. The sphere radii are close to the covalent radii of the atomic species involved. The resulting density of states was only weakly dependent on the radius chosen, within a range of several tenths of Angstroms around this radius.

Using the simplified (no 3*d* electrons) Ga pseudopotential, we have explicitly allowed for structural relaxation in the  $\text{Mn}_x\text{Ga}_{1-x}\text{N}$  structure, by allowing each atom to move under the forces exerted by the electrons and the other atoms. We found that the introduction of Mn had a non-negligible effect only on the position of the first shell of N neighbors, where the Mn-N bond length was elongated by a small 3%,

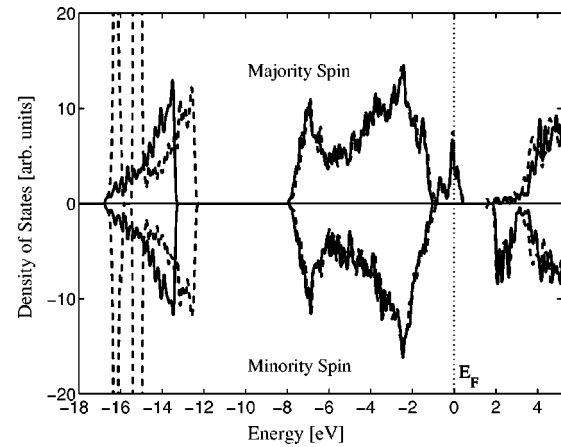


FIG. 1. Density-of-states curves for wurtzite  $\text{Mn}_{0.063}\text{Ga}_{0.937}\text{N}$ . Solid line: Ga 3*d* electrons treated as core electrons. Dashed line: Ga 3*d* electrons treated explicitly as valence electrons.

without destroying the tetrahedral symmetry. Subsequent shells were left unperturbed. The degree of bond elongation and the lack of perturbation to subsequent shells are in excellent agreement with recent x-ray-absorption fine-structure measurements.<sup>32</sup> A reduced coordination number consistent with Mn clustering was found experimentally, but is absent in our simulations of the ideally ordered alloy. As previously noted for  $\text{Mn}_x\text{Ga}_{1-x}\text{As}$  and  $\text{Mn}_x\text{In}_{1-x}\text{As}$ ,<sup>10</sup> the computed structural relaxation effects were small and were found to have negligible consequences on electronic and magnetic properties.

Our calculations find a global magnetic moment of  $4\mu_B$  per supercell. This value is in agreement with the magnetic moment of  $5\mu_B$  for the free Mn atom, which is reduced to  $4\mu_B$  in the lattice because the Mn impurity acts as an acceptor.

Calculations for the density of states performed at the relaxed  $\text{Mn}_x\text{Ga}_{1-x}\text{N}$  structural configuration without treating Ga 3*d* electrons, and at the unrelaxed  $\text{Mn}_x\text{Ga}_{1-x}\text{N}$  structural consideration with explicit treatment of Ga 3*d* electrons, are shown in Fig. 1. It is readily observed that the Ga 3*d* electrons do indeed interact with deep N 2*s* states, in agreement with Fiorentini *et al.*<sup>30</sup> However, it is clear that the effect of this interaction of the valence and conduction bands (as well as the effect of relaxation) is negligible. While the computed band gap is indeed smaller when Ga 3*d* electrons are considered explicitly, it is only smaller by an insignificant  $\sim 0.1$  eV. Therefore, all subsequent calculations were performed without explicit consideration of 3*d* electrons, which greatly simplified the numerical aspects of the computation.

In Fig. 1, both majority- and minority-spin components display a band gap, indicating that the introduction of Mn did not destroy the semiconducting nature of the material. The band gap is  $\sim 2.8$  eV. This value is somewhat higher than our computed value for pure GaN,  $\sim 2.4$  eV, due to the effect of Mn alloying. However, it is still lower than the experimental GaN band-gap value of  $\sim 3.4$  eV. This is reasonable, because density-functional theory is well known to underestimate semiconductor band gaps.<sup>25</sup> The most striking result of the introduction of Mn is the formation of a Mn-

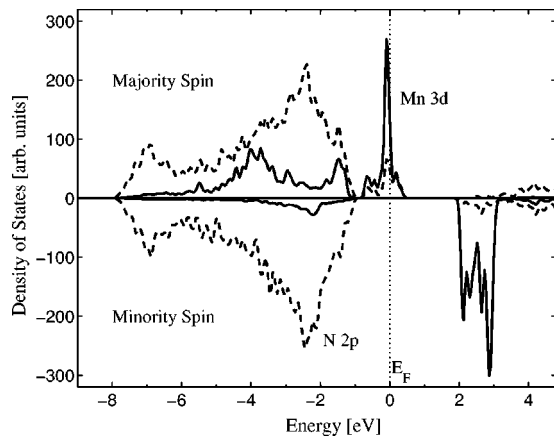


FIG. 2. Partial density-of-states curves for wurtzite  $\text{Mn}_{0.063}\text{Ga}_{0.937}\text{N}$ . Solid lines: Mn 3d. Dashed lines: N 2p.

related, *ideally spin-polarized* impurity band. This band is  $\sim 1.5$  eV wide, and is separated from the valence band by  $\sim 0.2$  eV. Importantly, the Fermi level is within the impurity band. Therefore, if charge carriers within it are sufficiently mobile, then carriers injected from the  $\text{Mn}_x\text{Ga}_{1-x}\text{N}$  layer will have ideal 100% spin-polarization. The introduction of Mn *did not* spin polarize the valence band noticeably, but caused a non-negligible spin polarization of the conduction band. These findings are in general agreement with the KKR-CPA results of Ref. 23, except for the vanishing semiconductor band gap in that study.

The above findings can be rationalized by means of partial DOS for the Mn 3d and N 2p orbitals (found to dominate the spin-polarization effects), given in Fig. 2. Clearly, the majority-spin impurity band is due to a broadening of the discrete Mn 3d impurity level, via hybridization with N 2p orbitals. It appears to be an intermediate case between two more extreme cases: the first is that of a discrete Mn-related level, found both theoretically<sup>21,24</sup> and experimentally<sup>33</sup> to be  $\sim 1$  eV to 1.5 eV above the valence-band edge in the isolated Mn impurity limit. The second is that of a spin-polarized feature that is indistinguishable from the valence band, previously found for a Mn concentration of  $x=0.25$ .<sup>22</sup> For the minority spin, Mn 3d levels with a much smaller degree of hybridization are found at the bottom of the conduction band. Turning to the valence band, the contribution of Mn 3d states to the majority spin is slightly larger than their contribution to the minority spin. However, their overall weight is negligible and the valence band is effectively nonpolarized.

The presence of a spin-polarized band *per se* is not a sufficient condition for efficient charge injection. An additional requirement is that charge carriers within the spin-polarized band are sufficiently mobile. To assess this, we calculated the band-structure diagrams. These are given in Fig. 3, where the bands are plotted for several high-symmetry directions in the Brillouin zone.

Figure 3 shows that we are still dealing with a direct band-gap semiconductor, as both the conduction-band minimum and the valence-band maximum are at the  $\Gamma$  point. But this semiconductor now contains a spin-polarized impurity band, which features a significant dispersion along some directions of the Brillouin zone. With the Fermi level running

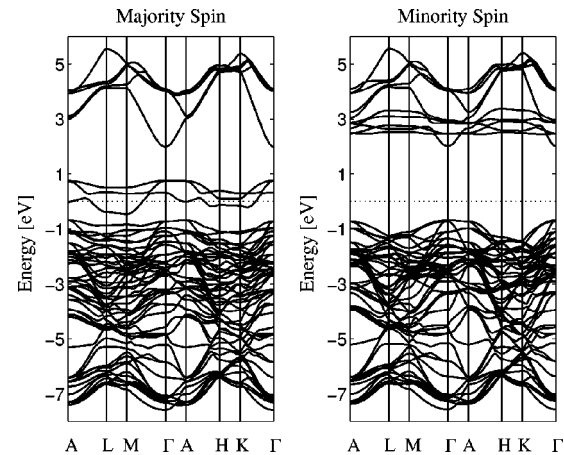


FIG. 3. Band-structure diagram along selected high-symmetry directions of the Brillouin zone of wurtzite  $\text{Mn}_{0.063}\text{Ga}_{0.937}\text{N}$ .

through this impurity band, we find that  $\text{Mn}_{0.063}\text{Ga}_{0.937}\text{N}$  is half metallic. It possesses a Fermi surface for the majority spin, but is devoid of one for the minority spin. This is clearly an *ideal* situation for spin injection, as 100% spin-polarized carrier injection may proceed by simple effective-mass transport in the impurity band.

Inspection of Fig. 3 reveals that the impurity band dispersion is negligible along the  $c$  axis of the Brillouin zone (e.g., along  $\Gamma$  to A or H to K), but is significant in the hexagonal plane (e.g., along A to L or M to  $\Gamma$ ). This is a direct result of the details of our supercell construction, which makes the distance between neighboring Mn atoms along the  $c$  axis larger than their distance on the hexagonal plane by the  $c/a$  ratio of 1.62. We conclude that the Mn-Mn in-plane distance of  $\sim 6.4$  Å produces significant hybridization, but the out-of-plane Mn-Mn distance of  $\sim 10.3$  does not. This provides a convenient lower and upper bound, respectively, for the minimal Mn-Mn distance required for obtaining significant impurity band dispersion. We note that for the minority spin, the non-hybridized Mn 3d orbitals seen in Fig. 2 are clearly manifested as nearly dispersion-free states in the conduction band. These states are useless for effective mass transport purposes and are merely localized Mn 3d states in resonance with the conduction band.

In practice, the position of the Fermi level is determined by “unintentional doping” of defects and residual impurities. If these effects are significant, “Fermi-level engineering,” performed by adding a different donor or acceptor species (in trace amounts, such that the band structure is not affected), may be required for bringing the Fermi level to within the impurity band. Such engineering need be done with care as it would also affect the free-carrier density and therefore the Curie temperature.<sup>11,20</sup> We stress that particular attention must be paid to the appropriate design of the interface, where the Fermi-level position may be significantly altered due to interface states.<sup>34</sup> In addition, the practical attainment of “pure” bandlike transport also depends on the degree of order in the material, with hopping conductivity increasing significantly at the expense of bandlike transport with increasing disorder.<sup>35</sup> As both defect and disorder effects are strongly growth and sample dependent, and do not affect our

discussion of the ultimate performance limits, they are not pursued further here.

It is very instructive to compare the present findings to a similar computation we have reported previously for zinc blende  $\text{Mn}_x\text{Ga}_{1-x}\text{As}$ , with the same Mn concentration of  $x = 0.063$ .<sup>10</sup> Interestingly, the behavior of  $\text{Mn}_x\text{Ga}_{1-x}\text{N}$  is not just quantitatively different from that of  $\text{Mn}_x\text{Ga}_{1-x}\text{As}$  (larger band gap), but is also strikingly different *qualitatively*. In  $\text{Mn}_x\text{Ga}_{1-x}\text{As}$ , the introduction of Mn caused a significant spin splitting of the valence band, a much smaller splitting of the conduction band, and did not result in an independent impurity band—the exact opposite of the present results. Physically, these sharp differences are due to the nature of the Mn impurity. In GaAs, Mn is a *shallow* acceptor, situated  $\sim 0.1$  eV above the valence-band maximum in the isolated impurity limit.<sup>36</sup> It therefore hybridizes primarily with the valence band, and completely merges with it for a few percent of Mn. In contrast, Mn is a deep acceptor in GaN—forming a level that is well over an eV above the valence-band maximum. Its interaction with the valence band is therefore much smaller and the introduction of Mn barely polarizes the valence band. For  $x = 0.063$ , the impurity band does not hybridize to an extent sufficient for merging with the valence band.

The different physics of Mn in GaAs and GaN may have profound practical implications. Whereas in GaAs the width of the 100% spin-polarized feature is small (bounded between 0.1 and 0.5 eV<sup>10,37</sup>), in GaN we find that it is  $\sim 1.5$  eV. This much increased width should result in much

greater immunity to both defect effects on the Fermi-level position and disorder effects on the band structure. We find that GaN is superior to GaAs not only in having an elevated Curie temperature, but also in having an electronic structure that is much more suitable for spin-polarized charge transport and potentially much more tolerant to technological limitations.

In conclusion, we have used density-functional-theory-based calculations to elucidate the electronic structure of ordered, ferromagnetic  $\text{Mn}_x\text{Ga}_{1-x}\text{N}$  with an experimentally realistic Mn content. Our physical conclusions were independent of whether Ga 3*d* electrons were considered explicitly or not. We found that  $\text{Mn}_x\text{Ga}_{1-x}\text{N}$  possesses a  $\sim 1.5$ -eV-wide impurity band, which is primarily due to hybridization of Mn 3*d* and N 2*p* orbitals. This band renders the material half metallic and supports effective-mass transport within it. This unique feature, together with the previously suggested high Curie temperature and inherent compatibility with GaN technology, makes  $\text{Mn}_x\text{Ga}_{1-x}\text{N}$  a potentially ideal material for spin-injection applications. If technological limitations can be overcome, it may emerge as a significant material for modern spintronic devices.

This work was supported in part by the National Science Foundation, the MRSEC Program of the National Science Foundation under Contract No. DMR-9809364, and the Minnesota Supercomputing Institute. We would like to thank Chris Palmström, Paul Crowell, Jun Lu, and Vitaliy Godlevsky for illuminating discussions.

- <sup>1</sup>S. Datta and B. Das, *Appl. Phys. Lett.* **56**, 665 (1990).
- <sup>2</sup>G. Prinz, *Science* **282**, 1660 (1998).
- <sup>3</sup>G. Burkard *et al.*, *Phys. Rev. B* **59**, 2070 (1999).
- <sup>4</sup>H. Ohno, *Science* **281**, 51 (1998), and references therein.
- <sup>5</sup>K. Takamura *et al.*, *J. Appl. Phys.* **89**, 7024 (2001).
- <sup>6</sup>For a recent review of device structures, see H. Ohno, F. Matsukura, and Y. Ohno, *Mater. Sci. Eng., B* **84**, 70 (2001).
- <sup>7</sup>B. Beschoten *et al.*, *Phys. Rev. Lett.* **83**, 3073 (1999).
- <sup>8</sup>Y. Ohno *et al.*, *Nature (London)* **402**, 790 (1999).
- <sup>9</sup>Y. Ohno *et al.*, *Physica E (Amsterdam)* **10**, 489 (2001).
- <sup>10</sup>M. Jain *et al.*, *Phys. Rev. B* **64**, 245205 (2001).
- <sup>11</sup>T. Dietl *et al.*, *Science* **287**, 1019 (2000).
- <sup>12</sup>See, e.g., S. Nakamura and G. Fasol, *The Blue Laser Diode—GaN Based Light Emitters and Lasers* (Springer-Verlag, Berlin, 1997).
- <sup>13</sup>M. Zajac *et al.*, *Appl. Phys. Lett.* **78**, 1276 (2001).
- <sup>14</sup>T. Szyszko *et al.*, *J. Cryst. Growth* **233**, 631 (2001).
- <sup>15</sup>S. Kuwabara *et al.*, *Physica E (Amsterdam)* **10**, 233 (2001); S. Kuwabara *et al.*, *Jpn. J. Appl. Phys., Part 2* **40**, L724 (2001).
- <sup>16</sup>M.E. Overberg *et al.*, *Appl. Phys. Lett.* **79**, 1312 (2001).
- <sup>17</sup>Y. Shon *et al.*, *Jpn. J. Appl. Phys., Part 1* **40**, 5304 (2001).
- <sup>18</sup>N. Theodoropoulou *et al.*, *Appl. Phys. Lett.* **78**, 3475 (2001); N. Theodoropoulou *et al.*, *Phys. Status Solidi B* **228**, 337 (2001).
- <sup>19</sup>M.L. Reed *et al.*, *Appl. Phys. Lett.* **79**, 3473 (2001); M.L. Reed *et al.*, *Mater. Lett.* **51**, 500 (2001).
- <sup>20</sup>V.I. Litvinov and V.K. Dugaev, *Phys. Rev. Lett.* **86**, 5593 (2001).
- <sup>21</sup>C.Y. Fong, V.A. Gubanov, and C. Boekema, *J. Electron. Mater.* **29**, 1067 (2000).
- <sup>22</sup>H. Katayama-Yoshida, R. Kato, and T. Yamamoto, *J. Cryst. Growth* **231**, 428 (2001).
- <sup>23</sup>K. Sato and H. Katayama-Yoshida, *Jpn. J. Appl. Phys., Part 2* **40**, L485 (2001).
- <sup>24</sup>M. van Schilfgaarde and O.N. Myrasov, *Phys. Rev. B* **63**, 233205 (2001).
- <sup>25</sup>See, e.g., J.R. Chelikowsky and M.L. Cohen, in *Handbook on Semiconductors*, edited by T.S. Moss, 2nd ed. (Elsevier, Amsterdam, 1992); W.E. Pickett, *Comput. Phys. Rep.* **9**, 115 (1989).
- <sup>26</sup>J. Perdew and Y. Wang, *Phys. Rev. B* **45**, 13 244 (1992).
- <sup>27</sup>N. Troullier and J.L. Martins, *Phys. Rev. B* **43**, 1993 (1991).
- <sup>28</sup>L. Kleinman and D.M. Bylander, *Phys. Rev. Lett.* **48**, 1425 (1982).
- <sup>29</sup>S.G. Louie *et al.*, *Phys. Rev. B* **26**, 1738 (1982).
- <sup>30</sup>V. Fiorentini *et al.*, *Phys. Rev. B* **47**, 13 353 (1993).
- <sup>31</sup>C. Stampfl and C.G. van de Walle, *Phys. Rev. B* **59**, 5521 (1999), and references therein.
- <sup>32</sup>Y.L. Soo *et al.*, *Appl. Phys. Lett.* **79**, 3926 (2001).
- <sup>33</sup>R.Y. Korotkov *et al.*, *Appl. Phys. Lett.* **80**, 1731 (2002).
- <sup>34</sup>W. Mönch, *Semiconductor Surfaces and Interfaces* (Springer-Verlag, Berlin, 1993).
- <sup>35</sup>N. Mott, *Conduction in Non-Crystalline Materials* (Oxford University Press, Oxford, 1987).
- <sup>36</sup>M. Linnarsson *et al.*, *Phys. Rev. B* **55**, 6938 (1997).
- <sup>37</sup>J. Szczytko *et al.*, *Phys. Rev. B* **59**, 12 935 (1999), and references therein.